ARTICLE

An SPR investigation toward the therapeutic drug monitoring of anticancer drug imatinib with selective aptamers operating in human plasma

Received 00th January 20xx,
Accepted 00th January 20xx

DOI: 10.1039/x0xx00000x

Stefano Tartaggia,[a,*] Anna Meneghello,[a,b] Ottavia Bellotto,[a,c] Ariana Soledad Poetto,[a,d] Martina Zanchetta,[a,c] Bianca Posocco,[a] David Bunka,[e] Federico Polo[a,b,*] and Giuseppe Toffoli [a]

The anticancer drug imatinib is often involved in therapeutic drug monitoring (TDM) studies aimed at improving the treatment of several forms of leukemia and gastrointestinal stromal tumors (GIST). To further implement the TDM of imatinib in the clinical practice, we developed a detection assay by using a ssDNA aptamer, which demonstrated an excellent selectivity and was not affected by interference from components of human plasma samples. The efficient binding of imatinib to the aptamer was demonstrated by means of surface plasmon resonance (SPR) analysis, which allowed the development of a quantitative assay in the concentration range between 400 and 6000 ng mL^{-1} (0.7-10 µM), where a lower limit of quantification (LLOQ) of 400 ng mL^{-1} was achieved. The precision of the assay was found within 12.0%, whereas the accuracy was in a range between 97.1 and 101.5%. The sample preparation procedure displayed a recovery in the range 48.8-52.8%. Solid validation data were collected according to regulatory guidelines and the method was compared with standard analytical techniques, leading to the development of a feasible aptasensor for the TDM of patients administered with imatinib.

Introduction

Imatinib (**1**) is an anticancer drug, widely used in the treatment of Philadelphia positive-chromosome chronic myeloid leukemia (CML),[1,2,3] acute lymphoblastic leukemia (ALL) and gastro-intestinal stromal tumor (GIST).[4,5,6] The antitumoral activity of imatinib relies on the inhibition of several tyrosine kinases, proteins such as ABL (encoded by the "Abelson leukemia" gene 1, *ABL1*) in CML, KIT (encoded by the "tyrosine kinase receptor" gene, *KIT*) and PDGFRA (encoded by the "platelet-derived growth factor receptor alpha" gene, *PDGFRA*) in GIST.[7] Imatinib strongly binds to tyrosine kinase receptors, preventing phosphorylation (transfer of phosphate groups from ATP) of the tyrosine residues on protein substrates and ultimately hampering the signal transduction necessary for cellular proliferation, which is abnormally activated in the malignant transformation process.[8]

Imatinib mesylate (Gleevec®) is administered to patients at an oral dose of 400 mg per day.[5] Upon administration, it is converted by cytochromes P450 3A4 and P450 3A5 primarily to N-desmethyl Imatinib (**2**), whose concentration is usually found at as much as 20-25% of the parent drug (Fig. 1).[9] Moreover, considering that a similar pharmacological activity for **1** and **2** was evidenced in previous studies, the implications of **2** in therapeutic drug monitoring (TDM) of imatinib is desirable as well.[10,11]

TDM is the clinical practice of measuring the plasma levels of therapeutic drugs at regular time intervals in order to maintain the drug concentration within the therapeutic window for any individual patient.

Imatinib (**1**) is often chosen as a model drug for TDM studies, as it has dramatically changed the management of several tumor diseases that are resistant to conventional cytotoxic chemotherapy.[12]

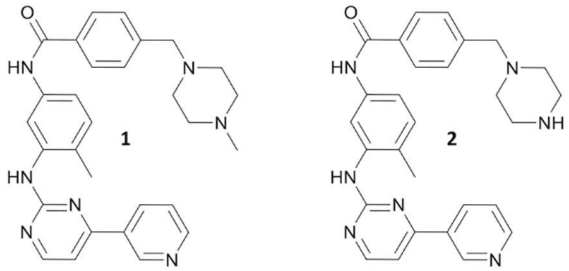

Fig. 1 Chemical structures of Imatinib (**1**) and N-desmethyl imatinib (**2**).

Indeed, the minimum plasma concentration (C_{min}), reached after successive administrations of Gleevec®, was correlated with the clinical response, as it exhibited a large inter-individual variability with a consistent dose–response relationship.[5] Several clinical trials demonstrated that threshold levels in plasma should exceed 1000 ng mL^{-1} (1.70 µM) and 1100 ng mL^{-1} (1.87 µM) to obtain clinical benefits in CML[13] and in GIST[7]

[a.] *Clinical and Experimental Pharmacology, Centro di Riferimento Oncologico di Aviano (CRO) IRCCS, Via Franco Gallini 2, 33081, Aviano, Italy. E-mail: stefano.tartaggia@cro.it*
[b.] *Current address Department of Molecular Sciences and Nanosystems, Ca' Foscari University of Venice, Via Torino 155B, 30172 Venezia, Italy. E-mail federico.polo@unive.it*
[c.] *Department of Chemical and Pharmaceutical Sciences, University of Trieste, Via Giorgieri 1, 34127, Trieste, Italy.*
[d.] *Department of Pharmacological and Pharmaceutical Sciences, University of Padua, Largo Meneghetti 2, 35131 Padova, Italy.*
[e.] *Aptamer Group, Suite 2.78 – 2.91, Bio Centre, Innovation Way, Heslington, York, YO10 5NY, UK.*
†Electronic Supplementary Information (ESI) available. See DOI: 10.1039/x0xx00000x

patients, respectively. Therefore, TDM is highly recommended in therapies involving imatinib, where C_{min} is the analytical parameter of interest that allows establishing a dose escalation to improve the therapeutic response or a dose reduction to prevent adverse effects during the administration of Gleevec®.[14]

To-date, standard analytical methods, employed to quantify **1** and its main metabolite (**2**) in clinical samples, rely on their simultaneous quantification by reverse-phase high-performance liquid chromatography (RP-HPLC) coupled with mass spectrometry.[15,16,11]

Research and development efforts aimed at miniaturizing analytical devices to enable point-of-care testing (PoCT), received an increasing amount of attention over the past decade. This is due to the advantages and benefits that TDM can provide as an established clinical practice to oncological patients.[17] In this context, sensing technologies enabling a precise, fast and reliable detection of the drug concentration levels in a small sample volume, ideally down to a single blood drop, are very promising.[18]

The main challenges to be addressed in the development of analytical devices and methodologies, can be summarized as follows. (i) A rapid and selective recognition of the analytical targets (especially small organic molecules), must be achieved without the need for significant pre-analytical treatment of patient samples. For example, HPLC-MS processes require expensive equipment in which the analytes are separated from interfering components before passing to the detection system (e.g. MS). (ii) Each proposed analytical method must be validated according to regulatory guidelines to provide quantitative information concerning the concentration of the therapeutic drugs and to help oncologists make crucial clinical decisions. (iii) Finally, using organic solvents to dilute and/or denature samples should be avoided to allow portable analyzers to be employed outside the centralized laboratories and core facilities. This may allow testing at patients' bedside, in medical practices or potentially at home.

Being a reference drug in TDM studies, several examples of non-conventional analytical methodologies for imatinib detection have been reported in literature. In particular, direct detection in clinical samples was described using electrochemical methods such as adsorptive stripping square-wave voltammetry. [19,20] This was successfully applied to the detection of **1** and **2** in urine. Recently, a label free detection approach based on surface-enhanced Raman spectroscopy (SERS) and multivariate calibration was also applied to human plasma samples, showing a good correlation with HPLC-MS data.[21] Specific antibodies for **1** were recently investigated and applied to develop an ELISA protocol, which was applied to serum samples from mice.[22,23]

Herein, we investigated the feasibility of detecting imatinib and its main metabolite at clinically relevant concentrations by means of a surface plasmon resonance (SPR) sensing platform employing a ssDNA aptamer as selective receptor in human plasma.

Aptamers are single-stranded nucleic acid oligomers which fold into selective 3D structures to form ligand-binding sites complementary in charge and shape to a specific target. Many aptamer-based applications have been demonstrated in the field of optical and electrochemical sensors.[24,25,26,27,28,29,30,31] Selective aptamers are available against a large number of targets and are usually selected and produced by external companies.[32]

Our investigation was performed by means of a SPR-based platform, which consists in a label-free optical detection methodology suitable to characterize the kinetic and steady-state affinity properties of biomolecular interactions. In general, the receptor molecule is immobilized at the sensor surface and the interaction with analyte molecules in solution, can be monitored in real time. A refractive index change is correlated to the mass change occurring at the sensor surface and is usually recorded as response units (RU). Although this technique is extensively applied to study large biomolecular systems (e.g. protein biomarkers and antibodies),[33] measuring the interactions between small molecules and aptamers or other biomolecular receptors is considered difficult. This is due to the small local change in mass density on the sensor surface which occurs when low molecular weight targets (<1000 Da) bind to heavier biomolecular receptor (typically >50000 Da).[34,35] The aim of our research work was to develop an analytical method to detect the small molecule and anticancer drug imatinib in human plasma, while relying on the use of a newly developed and specifically designed aptamer as the receptor of our biosensing platform. To this end, we exploited the Biacore X100, a robust SPR workstation that allowed us developing an analytical method that could be validated following the strict FDA regulatory guidelines to address the needs of oncologists and clinicians.

Experimental

Chemicals. Analytical reference standards of **1** (imatinib mesylate), PBS buffer, magnesium chloride ($MgCl_2$), calcium chloride ($CaCl_2$), formic acid and ammonium acetate, LC-MS grade isopropanol, imatinib-d8 and acetonitrile were purchased from Merk Sigma-Aldrich (Milan, Italy). N-Desmethyl imatinib (**2**) was purchased from Santa Cruz Biotechnology Inc (Dallas, TX, USA). Tween20 was purchased from VWR International S.r.l. (Milan, Italy). Imatinib aptamer (**3a**, 100-mer), 5'biotin imatinib aptamer (**3b**), 5'amino imatinib aptamer (**3c**), 5'thiol imatinib aptamer (**3d**) and 5'biotin immobilization oligomer (**4**, 15-mer) (see details in Supporting Information) were purchased from Aptamer Group (York, UK). Upon arrival, lyophilized oligomers were solubilized with milli-Q water, aliquoted and stored at -20°C. Co-medications for selectivity tests, in particular telmisartan (**5**), lansoprazole (**6**), tamsulosin (**7**), finasteride (**8**), lisinopril (**9**), pravastatin (**10**) were purchased from Merk Sigma-Aldrich. Amlodipine (**11**), paracetamol (**12**), furosemide (**13**), enalapril (**14**), hydrochlorothiazide (**15**) and allopurinol (**16**) were provided by the pharmacy of the *Centro di Riferimento Oncologico di Aviano*, Italy. The chemical structures of the co-

medications are reported in the Supporting Information, Table S1. Control human plasma stabilized with K_2EDTA for the preparation of daily standard calibration curves and quality control (QC) samples, was obtained from healthy volunteers and was provided by the Transfusion Unit of the *Centro di Riferimento Oncologico di Aviano*, Italy. The analytes, aptamers and co-medications employed in this work to develop the SPR biosensing platform are summarized in **Table 1**.

Table 1. Summary of the analytes, comedications and aptamers used in this work

Compound	Name	Role
1	Imatinib mesylate	Main analyte
2	N-Desmethyl imatinib	Co-analyte
3a	Imatinib aptamer (100-mer)	Capturing of **1** (and **2**)
3b	5'biotin imatinib aptamer	Capturing of **1** (and **2**). Tethered to the streptavidin-functionalized surface of SPR chip
3c	5'amino imatinib aptamer	Capturing of **1** (and **2**). Covalently bound to the carboxylic acid-functionalized surface of SPR chip
3d	5'thiol imatinib aptamer	Capturing of **1** (and **2**). Covalently bound to the maleimide-functionalized surface of SPR chip
4	5'biotin immobilization oligomer (15-mer)	Binding of **3** (a, b, c or d). Tethered to the streptavidin-functionalized surface of SPR chip
5	Telmisartan	Co-medication
6	Lansoprazole	Co-medication
7	Tamsulosin	Co-medication
8	Finasteride	Co-medication
9	Lisinopril	Co-medication
10	Pravastatin	Co-medication
11	Amlodipine	Co-medication
12	Paracetamol	Co-medication
13	Furosemide	Co-medication
14	Enalapril	Co-medication
15	Hydrochlorothiazide	Co-medication
16	Allopurinol	Co-medication

Aptamer selection. Selection of the aptamers against imatinib was carried out by Aptamer Group (York, UK) according to the company's 'Displacement Selection' approach, which was extensively developed and automated, based on previously reported methods.[36,37] Aptamer **3a** was selected among a pool of sequences as the best candidate to bind **1**, as described in details in the Supporting Information. Further modifications of **3a** at the 5'-end with a 6-carbon linker bearing specific functional groups, namely biotin, amino and thiol, provided the related functional aptamers against imatinib: **3b** (5'-biotin), **3c** (5'-amino) and **3d** (5'-thiol), respectively (see Table 1). Details and sequences regarding the aptamer **3a-d** selection process and concerning the use of oligomer **4**, which is a shorter sequence binding to the aptamer in a hybridization region within the molecule, can be found in the Supporting information and in the recently accepted patent.[38]

SPR measurements. SPR measurements were performed using a Biacore X100 workstation (GE Healthcare Life Sciences), at 25 °C, with a flow rate of 5 and 10 μL min^{-1}. Streptavidin coated sensor chips (SA) and running buffer (HBS-EP+) were purchased from GE Healthcare Life Sciences (Milan, Italy). The SPR system allows a differential measurement as the sample passes sequentially over two flow cells. The first flow cell (FC1) lacks the receptor and acts as the reference, while the second flow cell (FC2) contains the receptor. The signal resulting from the difference in response of the two flow cells (FC2-FC1) provides the information concerning the desired interaction, thus excluding non-specific interactions and any interference generated by refractive index changes due to mixing phenomena or variations in the experimental conditions, such as density, viscosity and pressure.

Binding analysis. The immobilization of **3b** onto the SA chip, as schematically shown in Figure S1, occurs as it follows. After conditioning the surface of a SA chip with a mixture of 50 mM NaOH and 1M NaCl (3 x 1 min), **3b** (5 μM) in PBS buffer (25 mM, pH 7.2) was injected for 240 s at 10 μL/min over FC2 only. PBS buffer (25 mM, pH 7.2) containing 0.05% Tween20 was used as the running buffer. The system was finally washed with a mixture of 50% isopropanol in 50 mM NaOH and 1M NaCl. The immobilization process yielded 2713 RUs of **3b** (Fig. S2). Binding analysis was performed on the SA chip functionalized with biotinylated aptamer **3b**, using twelve imatinib dilutions (from 0.021 to 1.26 μM) in PBS buffer (10 mM, pH 6,0) containing NaCl (100 mM), KCl (2 mM) $MgCl_2$ (5 mM), $CaCl_2$ (2 mM) and Tween 20 (0.05%). Flow rate was set at 30μL/min and association and dissociation time were both 180 s. A blank sample (0 nM) was included. Regeneration between each imatinib injection was performed with H_2O. All sensorgrams were corrected by subtracting the signal recorded in FC2 (functionalized cell) from the signal recorded in FC1 (reference cell); FC2-FC1 data were double referenced by blank (0 nM sample) signal subtraction. Collected data were evaluated by non-linear analysis of the association curves using SPR kinetic evaluation software (BIAevaluation Software, version 2.0.2 Plus Package, Biacore). Data fitting was carried out according to a 1:1 steady state approximation model to obtain K_D. Fitting analysis was evaluated for all the performed assays and was compliant to the following statistical parameters: χ^2 < 5% of R_{max} and SE (standard error) values < 10% of the corresponding parameters.

Concentration analysis in buffered media. The immobilization of **4** onto the SA chip, as schematically shown in Fig. S1, occurs as it follows. After conditioning the surface of a SA chip with a mixture of 50 mM NaOH and 1M NaCl (3 x 1 min), **4** (5 μM) in PBS buffer (25 mM, pH 7,2) was injected for 240 s at 10 μL/min over FC1 and FC2. Standard HSB EP+ buffer (GE) was used as the running buffer. The system was finally washed with a mixture of 50% isopropanol in NaOH 50 mM and NaCl 1M. The immobilization process yielded 2084 and 2007 RUs of **4** in FC1 and FC2, respectively (Fig. S3). Aptamer **3a** (1.2 μM) in PBS buffer (50 mM, pH 7.2) containing NaCl (685

mM), KCl (13,5 mM) $MgCl_2$ (5 mM) and $CaCl_2$ (2 mM), named 'hybridization buffer', was injected over 540 s into the FC2 housing the SA chip functionalized with **4**. After 300 s of stabilization time, imatinib standards were injected over 420 s on both flow cells. Experiments were performed at a flow rate of 10 µL/min using PBS (25 mM, pH 7.2) containing NaCl (342 mM) and KCl (6.75 mM) as the running buffer with 6 calibration standards of **1** from 50 to 500 ng mL^{-1} in PBS buffer (10 mM, pH 6,0) containing NaCl (100 mM), KCl (2 mM) $MgCl_2$ (5 mM), $CaCl_2$ (2 mM). Surface regeneration was performed with a mixture of 8 mM NaOH and 160 mM NaCl for 20 s. A blank sample (0 ng/mL) was always included.

Concentration analysis in human plasma

Standards and quality control working solutions. A stock solution of imatinib mesylate at 1000 µg mL^{-1} was prepared in DMSO and stored at -20 °C. A series of working solutions ('a' to 'g'), used to prepare calibration standards and quality control (QC) samples at low (QCL), medium (QCM) and high (QCH) concentrations were obtained by diluting the stock solution with DMSO to the concentrations reported in Table S2 (Supporting Information). Aliquots of these solutions were kept in Eppendorf polypropylene tubes at -20 °C and used for a maximum of five freeze-thaw cycles.

Preparation of standards and quality control samples. A seven-point calibration curve was newly recorded every day during this study. Each calibration and QC sample was freshly prepared by adding 1.25 µL of working solution from 'a' to 'g' in 23.75 µL of pooled blank human plasma in a 0.5 mL Eppendorf polypropylene tube to obtain the final concentrations reported in Table S2 (Supporting Information). Each calibration curve included a blank and three QC samples, which were analyzed in triplicate. The calibration standards and QCs were diluted with 350 µL of PBS buffer (12 mM, pH 5.6) containing NaCl (103 mM), KCl (2 mM) $MgCl_2$ (6 mM), $CaCl_2$ (2 mM) and Tween 20 (0.05%), named as 'incubation buffer', and thoroughly vortexed for 10 seconds three times. The content of each tube was transferred on a centrifugal filter (Millipore Amicon® Ultra 0.5 mL, 50 KDa cut off) and centrifuged at 8000 rpm for 15 min at 25 °C. Then, 330 µL of the filtrate were transferred on 11 mm plastic vials (Scheme S1, Supporting Information) and analyzed as described below.

Concentration analysis. Experiments were performed with the SA chip functionalized with **4**, as described above, using PBS (25 mM, pH 7.2) containing NaCl (342 mM), KCl (6.75 mM) and Tween 20 (0.05%) as the running buffer. For each run, **3a** (1.2 µM) in the hybridization buffer was firstly injected in FC2 for 600 s at 5 µL/min. Imatinib standards, prepared as described above, were injected in both flow cells after 300 s of stabilization time at 10 µL/min for 420 s in the following order: blank, calibration standards, QCs in triplicate and unknown samples. The chip surface was regenerated after each injection with a mixture of 8 mM NaOH and 160 mM NaCl for 20 s. The regression analysis to establish the dose-response relationship was performed with the software OriginPro 2019b (OriginLab, Northampton, MA, USA).

Validation study. This study was carried out by taking into account recommendations of the U.S. Food & Drug Administration (FDA) for ligand-binding assays (LBA) validation.[39] The following parameters were evaluated to validate the method: recovery, intra- and inter-day precision and accuracy, reproducibility, lower limit of quantification (LLOQ), selectivity and matrix effects (see Supporting Information for full details).

Mass Spectrometry. Quantification of imatinib in plasma samples collected from patients undergoing therapeutic regimen was performed by using tandem mass spectrometry, as the reference method to assess the quality of the SPR assay. The analysis was conducted with an API 4000 QT (Sciex) working in multiple reaction monitoring (MRM) mode and preceded by a Shimadzu LC system. The procedure and operative conditions were similar to those previously reported by our group.[11] Briefly, a 5 µL aliquot of each calibrator, QC and unknown samples was transferred to a clean polypropylene tube and mixed with 245 µL of a methanolic solution containing the internal standard imatinib-d_8 at 10 ng mL^{-1} (0.017 µM) to perform plasma protein precipitation. After vortexing and centrifugation at 16000 g at 4 °C for 10 min, the supernatant was transferred to an autosampler vial for analysis. Chromatographic separation was performed on a Synergi Fusion-RP column (4 µm, 80 Å, 50 x 2.0 mm) in solvent gradient. At time t_0 = 0 the mobile phase A (2 mM ammonium acetate and formic acid 0.01% in water) was run into the column; at t_1 = 3.02 min the solvent gradient was changed to 90% A and 10% B (80% acetonitrile, 20% isopropanol and 0.1% formic acid); at t_2 = 5.99 min B was increased to 60% , while it was kept constant at 98% between t_3 = 6.2 min and t_4 = 7 min. At t_5 = 7.49 min, B was reduced to 2% and kept at the same ratio until the end of the run, at t_6 = 8.5 min. Flow rate was 0.45 mL/min, except between 1.49 and 3.03 min, where it was fixed at 0.4 mL min^{-1}. Column temperature was set at 50 °C and the injection volume was 2 µL. The ESI source was set to positive ion mode and the selected transitions for the quantification of analytes were 494.4 to 394.2 and 480.4 to 394.2 m/z for **1** and **2**, respectively.

Ethics statement regarding human samples. Patient's samples were collected within a clinical study (CRO-2017-19, EudraCT number: 2017-002437-36) approved by the local ethics committee (Comitato Etico Unico Regionale- C.E.U.R.) and by Agenzia Italiana del Farmaco (AIFA, Rome, Italy), which was conducted according to the principles expressed in the Declaration of Helsinki. Informed consent was obtained from all participants involved in the study.

Results and discussion

The aptamers for imatinib **3a-d** and related complementary oligomer **4** were first tested to assess their properties and optimize experimental conditions to develop a quantitative bioassay. Preliminary experiments to functionalize the chip surface were attempted by means of common immobilization strategies with aptamers bearing a 6-carbon linker ending with biotin (**3b**), amino (**3c**), thiol (**3d**) functional groups at the 5' end. Although successful protocols for immobilization of amino or thiol modified receptors on the carboxylated dextran of CM5[35] or bare gold chip[40] were reported in the literature, these approaches led to poor immobilization and hybridization yields for our purposes (in general below 300 RUs) and could not be efficiently employed for further investigations. Details concerning the immobilization procedures adopted for **3c** and **3d**

aptamers are provided in the Supporting Information along with the related sensorgrams (Fig. S4 and S5). Instead, the simple injection of a 5 µM solution in PBS buffer of **3b** or **4** on a streptavidin coated chip (see Supporting information, Fig. S1) provided high immobilization levels. In fact, ca 2000 and 2700 RUs were achieved for **4** and **3b** respectively (see Supporting Information, Fig. S2 and S3) on the sensor surface.

Affinity studies. When a small molecules (low MW) binds to a receptor (high MW) immobilized on a SPR sensor surface, the change of the refractive index or the local value of dielectric constant at the interface (receptor-functionalized surface/solution) may be low; compared with that caused by the immobilization of the receptor on the sensor surface. Therefore, it may not provide a detectable change of reflectivity and thus a measurable SPR signal. However, injection of imatinib solutions in PBS buffer at increasing concentrations over the aptamer immobilized on the sensor chip provided a typical association/dissociation response as shown in Fig. 2a. The shape of the sensorgrams related to this interaction display the classical behavior in which both association and dissociation of the substrate (**1**) and the ligand (**3b**) are fast processes. After injecting imatinib solutions at a flow rate of 30 µL/min, the response quickly achieved a plateau, enabling the evaluation of K_D by fitting the steady state affinity curve with a 1:1 binding model (Fig. 2b, BIAevaluation Software, version 2.0.2 Plus Package, GE). Despite the low intensity of the signal, the data analysis provided a K_D of 131 ± 11 nM, which is in a typical range for small molecule binding.[35]

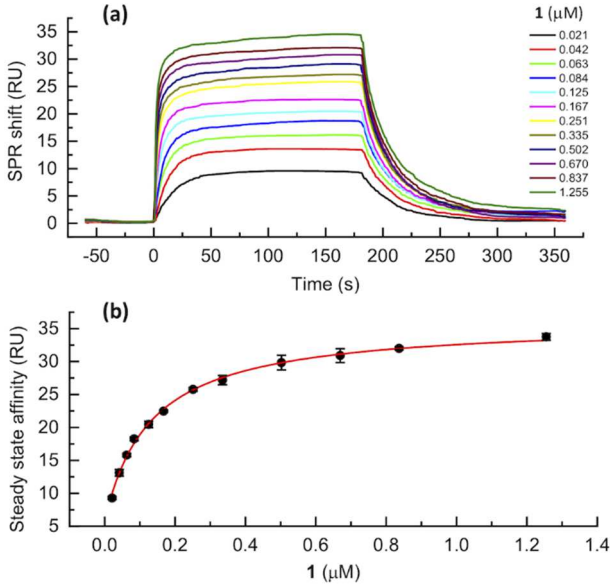

Fig. 2 (a) blank subtracted sensorgrams and **(b)** steady state affinity curve obtained after injecting imatinib solutions in the concentration range 0.021 - 1.26 µM in PBS buffer (10mM, pH 6,0) containing $MgCl_2$ (5 mM), $CaCl_2$ (2 mM) and Tween 20 (0.05%) on the SA chip functionalized with **3b**. Each data point is referred to measurements in triplicate.

Calibration strategy. The affinity study showed that a SPR response, arising from the direct binding of **1** with the aptamer, was achieved. However, the signal was relatively low in PBS. Therefore, one may ask whether the response of the bioassay could be further affected when running a real sample. For this reason, we investigated another strategy to develop the bioassay, which was based on the SA chip modification with **4** followed by the duplex formation with **3a** and subsequent injection of imatinib solutions at different concentrations (Fig. 3). Our hypothesis was that aptamer displacement in the presence of imatinib would have significantly greater SPR response in view of developing a quantitative assay operating in complex biological matrices for TDM applications. In fact, the conformational change occurring in the presence of **1** was expected to release the aptamer from the duplex structure, thus generating a suitable signal for the analytical measurement.[37]

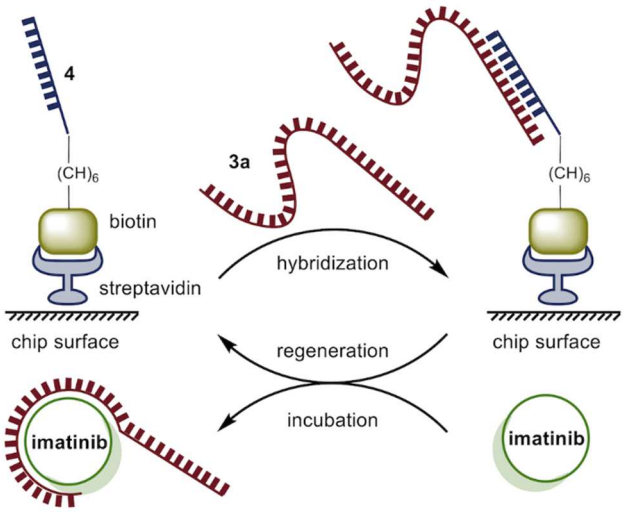

Fig. 3 Schematic representation of the aptamer-based assay for the detection of imatinib. After hybridization of **3a** with **4** immobilized on SA chip, imatinib solutions were injected, leading to the release of **3a** from the surface and the generation of a SPR response suitable for analytical quantification.

Preliminary investigations to optimize the hybridization of the aptamer **3a** toward **4** immobilized on SA sensor chip were carried out. Injection of the aptamer in 50 mM PBS (hybridization buffer) over the sensor surface for 540 s at 10 µL/min or 600 s at 5 µL/min led to a satisfactory coverage of **3a** on the surface. Instead, complete dissociation of **3a** was obtained upon injection of a mixture of 8 mM NaOH in 160 mM NaCl for 20 sec. This washing allows the platform to be regenerated and reused after each experiment. We also found similar hybridization levels by injecting **3a** in the concentration range from 1 to 2 µM on a new chip. Therefore, we preferred using the lower amount possible of aptamer to reduce its consumption. However, the aptamer concentration was increased to 1.2 µM to compensate the chip degradation, which occurred with the increasing numbers of runs. In fact, even though the hybridization yield varied from 1100 to 1200 RUs while using different SA chips; it maintained an excellent reproducibility on the same chip. Indeed, a CV of 2% was usually maintained after the first 200 experiments in a typical life cycle of a single SA chip, while a 15% loss in activity occurred during the following 200 runs, due to surface degradation. Only FC2 was functionalized with the aptamer; FC1 was used as reference cell to correct for non-specific interactions.

After hybridization of the aptamer over immobilized **4**, imatinib solutions were injected over both flow cells. Dissociation of aptamer from FC2 was observed as a decrease in the SPR signal, proportional to the concentration of imatinib. The PBS buffer (10 mM at pH 6) was used to dilute **1**, analogously to that utilized for selection process. However, its composition was

optimized for the development of the analytical method by recording the SPR response at 50, 200 and 500 ng mL^{-1} (0.09, 0.34, 0.85 µM, respectively) of **1** while varying the concentrations of $MgCl_2$ and $CaCl_2$ in the buffer (see Supporting Information Fig. S6). Specifically, $MgCl_2$ was tested in a range from 2.5 to 10 mM and an optimal concentration of 5 mM was determined, especially at 50 ng mL^{-1} (85 nM) of **1**. Instead, $CaCl_2$ was evaluated from 0 to 5 mM and displayed an optimal response at 2 mM. Therefore, a 10 mM PBS at pH 6 containing 5 mM $MgCl_2$ and 2 mM $CaCl_2$ was chosen for the incubation.

The sensorgrams corresponding to each injection of imatinib were double referenced, firstly by subtracting the response of FC1 (reference cell) from FC2, to provide data as shown in Fig. 4a. Secondly, a further correction was performed by subtracting the blank 'target-free' sample from each non-zero sample and flipping data to plot the aptamer dissociation as a positive response (Fig. 4b). ΔRU (RU_{sample} - RU_{blank}) was evaluated 200 s after the stop of each sample injection, while sampling the signal from 1700 to 1750 s (from run start). The results showed a linear response in simple buffer matrix in the concentration range of 50 to 500 ng mL^{-1} (0.09-0.85 µM) of **1** (Fig. 4c).

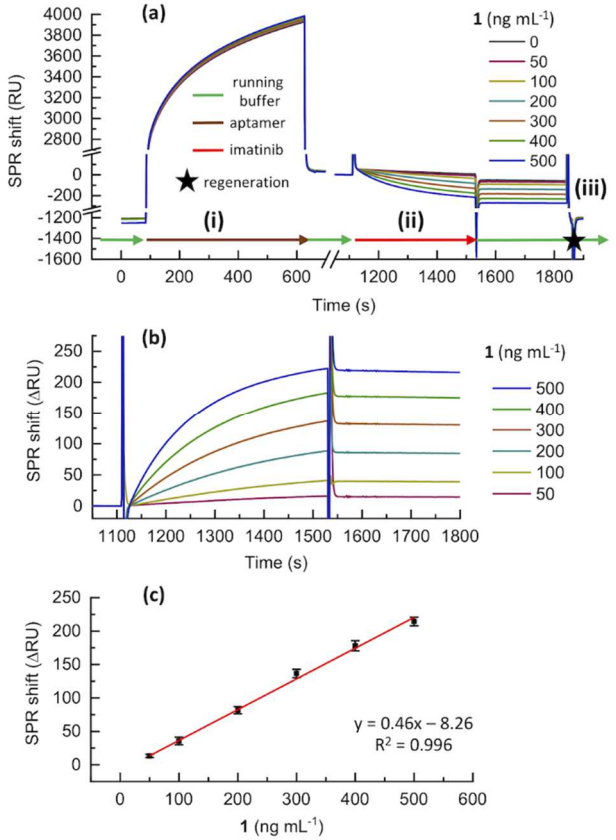

Fig. 4 (a) Sensorgrams for the overall calibration experiment (FC2-FC1). The three regions can be summarized as it follows: (i) aptamer hybridization on the sensor chip surface, (ii) sample incubation and (iii) regeneration of the chip for the next run. **(b)** Dissociation of aptamer from the surface. The data were obtained by subtracting the sensorgram of the blank (corresponding to 0 concentration) and then flipped to plot the results as a positive response. **(c)** Calibration curve obtained by plotting ΔRU values, collected 200 s after the end of sample injection, against the concentration of **1**. Experiments were carried out in triplicate.

Unfortunately, the process deviated significantly from linearity at higher concentrations. The detection limit in buffered media was evaluated by analyzing the blank variability, according to LOD = $3*SD_b/m$, where SD_b is the standard deviation of the blank and m is slope of calibration curve, providing a LOD of 3.2 ng mL^{-1} (5.4 nM).

Imatinib detection in human plasma. Once the feasibility of the outlined strategy had been shown to reliably detect and quantify **1** by employing **3a** hybridized to the SPR platform functionalized with **4**, a further effort was needed to develop a methodology for the quantification of **1** in plasma samples. Unlike simple buffered media, human plasma is a complex matrix with a high protein content, especially albumin and α-glicoproteins, which are known to bind 90-95% of imatinib.[41,42]

Moreover, direct injection of plasma samples into the flow cells of Biacore X100 instrument resulted in a consistent binding of the plasma components to the sensor surface, leading to an irreproducible SPR response with the additional risk of severe damages to the sensor surface and to the microfluidics of the instrument.

A 1:10 and 1:15 dilution step were investigated to match the instrumental linear response, previously obtained between 50 and 500 ng mL^{-1} (0.09-0.85 µM) in buffer media, with the clinically relevant concentration of **1** in plasma samples, whose range is from 1000 ng mL^{-1} (1.7 µM, C_{min} for CML patients) to 3500 ng mL^{-1} (5.9 µM).[43]

A PBS buffer containing 6 mM $MgCl_2$ and 2 mM $CaCl_2$ was used as incubation buffer to dilute the samples. Unfortunately, even diluted plasma was not suitable for SPR analysis, as plasma proteins still resulted in a huge SPR shift due to their adsorption on the sensor surface, obscuring the aptamer dissociation process (see Fig. S7 in the Supporting Information for details). To avoid the response of the large protein content, a further step of microfiltration by employing 50 KDa centrifugal filters was included. In this case, sensorgrams appeared completely free of non-specific binding by proteins and were similar to those previously recorded in simple buffer media (Fig. 4a). However, imatinib response was still too low and a calibration curve could not be obtained. This could be reasonably ascribed to the binding of imatinib to plasma proteins, which prevented enough recovery of unbound imatinib in the filtrate. To address this issue, the addition of Tween 20 in the buffer used to dilute plasma samples successfully reduced non-specific binding (NSB) related to protein-drug interactions in plasma. Other surfactants (e.g. sodium dodecyl sulfate or cetyl trimethyl ammonium bromide) or standard dextran NSB reducer[44] (from GE) did not provide significant recovery from plasma. The amount of Tween 20 in the buffer was adjusted to 0.05% after testing different amounts of the surfactant.

During our investigation, we found that at least 15 and 12 mM PBS was necessary to dilute plasma 1:10 and 1:15 respectively to maintain a pH of 6. Interestingly, we found a higher SPR response using the 1:15 dilution at each standard concentration, which was due to the increased aptamer dissociation occurring in a more diluted buffer even in the presence of a lower final concentration of analyte. Moreover, a

1:15 sample dilution allowed a minimum plasma volume of 25 µL for the SPR analysis and reduced those biological interferences that would have affected the measurement using lower dilution factors.

Contrary to the simple buffer media, the correlation of SPR response against concentration of **1** in plasma required a 4 parameter logistic (4PL) model to properly fit the calibration points,[45] as suggested also by LBA validation guidelines (see Supporting Information for a brief description of the model).[39]

Finally, once the procedure to prepare plasma samples for SPR analysis was optimized; a quantitative assay was set up to verify the full potential of the aptamer-based assay for the quantification of **1** and its main metabolite **2** for TDM applications. The recommendation and guidelines of FDA[39] were taken into account to validate our methodology as described in the following section.

Recovery. As described above, the preparation of samples was based on 1:15 dilution of plasma samples with incubation buffer followed by microfiltration with 50 KDa cut-off centrifugal filters (Scheme 1). The recovery of imatinib from microfiltration procedure, evaluated in three replicates at three QC concentrations, was in the range 48.8 – 52.8% with CV ≤ 8.8% (Table 1). The recovery of our method was evaluated by means of the efficiency of centrifugal microfiltration procedure and indicates the amount of **1** found in the filtrate, with respect to the theoretical quantity spiked in the sample. Although a significant loss of the analyte occurred during the microfiltration, both calibration standards and samples were processed following the same procedure to simulate the processing of real samples as much as possible. This was confirmed by preparing calibration standards with independent stock solutions of imatinib, other than those utilized for QCs. The back-calculated concentrations allowed determine the intra- and inter-day accuracy and precision as described in the following sections.

Calibration curves. Accuracy and precision data for each standard were evaluated on six calibration curves recorded in different days and summarized in Table 2. After processing sensorgrams as described above, the response was plotted against the nominal concentration of the analyte (undiluted plasma samples) to generate calibration curves through a 4PL regression (Fig. 5a). A linear fitting with acceptable back-calculated concentrations was obtained in the concentration range of 400 to 6000 ng mL^{-1} (0.7-10 µM), as shown in Fig. 5a. Pearson's coefficient of determination (R^2) was higher than 0.995 for each set of measurement, while the accuracy was between 97.1% and 101.8% and the precision, expressed as CV%, ranged from 1.3% to 5.2%.

Calibration curves in plasma were corrected for the dilution factor (1:15) and compared with those obtained in buffer (see Supporting Information, Fig. S8). Even though the working range for both matrices is almost the same, a slightly higher sensitivity was observed in buffer. This is mainly due to the recovery of centrifugal microfiltration procedure that limited the sensitivity of the method in plasma.

Intra-day and inter-day precision and accuracy and reproducibility. Precision and accuracy of the method were evaluated using QC samples (750, 2500, 4500 ng mL^{-1}) in triplicate within a single-set analysis for intra-day and in triplicate over six sets of measurements for inter-day assessment. The intra- and inter-day precision (CV%) were in the range 1.7-8.4% and 2.0-7.9%, respectively. Moreover, the method showed intra- and inter-day accuracy within the range 99.9-101.1% and 99.0-100.4% (Table 2).

Table 2 Summary of the validation data for the SPR analysis of imatinib in plasma. Standards and QCs were prepared according to Scheme S1.

Entry	N. C. (ng mL^{-1})	Mean B. C. ± SD (ng mL^{-1})	Precision (%)	Accuracy (%)
calibration curves	400	405 ± 10	2.5	101.2
	1000	991 ± 30	3.0	99.1
	2000	1979 ± 68	3.4	99.0
	3000	3054 ± 158	5.2	101.8
	4000	4043 ± 128	3.2	101.1
	5000	4857 ± 121	2.5	97.1
	6000	6077 ± 81	1.3	101.3
Intra-day	750	749 ± 63	8.4	99.9
	2500	2528 ± 74	2.9	101.1
	4500	4525 ± 75	1.7	100.6
Inter-day	750	747 ± 59	7.9	99.6
	2500	2476 ± 106	4.3	99.0
	4500	4519 ± 88	2.0	100.4
Matrix effect	400	406 ± 48	12.0	101.5
Nor-imatinib	750	693 ± 42	6.1	92.4
	2500	2217 ± 19	0.9	88.7
	4500	4351 ± 47	1.1	96.7
		Recovery (%) ± SD	CV %	
Recovery	750	48.8 ± 3.3	6.7	
	2500	51.7 ± 2.0	3.9	
	4500	52.8 ± 4.7	8.8	
LLOQ = 400 ng mL^{-1}				

N. C. = nominal concentration; B. C. = back calculated concentration.

Lower limit of quantification (LLOQ) and matrix effect. Taking into account that a spontaneous dissociation of **3a** from the sensor surface was occurring to some extent in the buffer used for incubation with the drug, aptamer dissociation due to the interaction with **1** was obtained by subtraction of the response from a blank sample. According to guidelines, a bias of up to 25% is allowed at the LLOQ level.[39] However, a tighter bias was suggested to be beneficial when fitting a model to the standards.[45] To asses LLOQ, eight independent replicates for each standard were analyzed by plotting biases against concentration. Biases were within 10% for all calibrators except at 400 ng mL^{-1} (0.7 µM), in which a 20% value was found. Therefore, it was considered appropriate as the LLOQ and the lowest standard of the calibration curve (see Supporting Information, Fig. S9). As a consequence, this method can be applied to the entire therapeutic range to evaluate imatinib concentration below the C_{min} and to detect toxic dosage of the drug, usually above 3000 ng mL^{-1} (5 µM).[46] To check possible

interference by plasma components or other interference in the sample, aliquots of plasma from eight different donors were spiked with **1** at the lowest calibrator. The quantification through a calibration curve prepared with pooled plasma provided the same back calculated concentration at 400 ng mL^{-1} (0.7 µM) with precision of 12.0% and accuracy of 101.5%. Moreover, the co-medications **5** to **16**, commonly associated with the administration of **1**, gave no interference at all in terms of additional interaction with **3a** hybridized on the chip surface (see Supporting Information, Table S2 and Fig. S10). The LOD of the method was estimated on six replicates of the blank, which were analyzed within a single set analysis. Therefore, the analysis of the blank variability (3*SD_b), with the 4PL model, provided a LOD of 79.5 ng mL^{-1} (0.13 µM) in plasma.

As a final remark, we can further confirm that the quantification of **1** through the optimized aptamer displacement approach was a better strategy, when compared to the direct detection approach. In fact, for the latter one, showing an aptamer immobilization level of 2700 RU, the response range of **1** was found in a range from 9 to 34 RUs, as shown in Fig. 2. Instead, the optimized aptamer displacement approach, provided responses in a range from 13 to 214 RUs in buffer media (Fig. 4b) and 12 to 132 RUs in plasma (see next sections and Fig. 5a), thus enhancing the sensitivity of about 4 to 6 times, with excellent precision and accuracy data, as shown below in the validation study.

Response of N-desmethyl imatinib. Detection of **2** was also tested on three QC samples at 750, 2500 and 4500 ng mL^{-1} (1.3, 4.2 and 7.6 µM, respectively). The SPR response was evaluated using the calibration curve obtained for imatinib standards. The back calculated concentrations were almost identical to those obtained for QC samples containing **1** and showed CV < 6.1% and accuracy between 88.7 and 96.7%. A comparison of SPR determination of **1** and **2** in spiked human plasma is shown in the Supporting Information, Fig. S11. The results clearly demonstrated that the aptamer could not discriminate between **1** and **2**, which is not surprising as there is no substantial difference in their chemical structures. This evidence provides both advantages and disadvantages. In fact, the main drawback is that both compounds are detected simultaneously unless a suitable separation system, such as chromatography, is used before the sample reaches the sensor. However, one should keep in mind that both compounds exploit the same antitumor activity and that, from a clinical point of view, it is important to determine the total concentration of active drug, being **1**, **2** or both. Although further investigations on their simultaneous quantification for TMD purposes are needed, this is the first time, to the best of our knowledge, that a biosensing approach is employed to develop an analytical method to detect **1** and **2** with accuracy and precision data suitable for analytical validation in clinical samples.

Comparison of the SPR assay with HPLC–MS. Our findings showed promising validation data when utilizing aptamer **3a** to detect **1** and **2** in human plasma, including excellent linearity, recovery, selectivity, low matrix effect, inter- and intra-day precision and accuracy values. Therefore, our protocol was finally tested on 12 available samples, taken from patients administered with imatinib at the *Centro di Riferimento Oncologico di Aviano,* Italy) which were also analyzed *via* HPLC-MS. The samples were processed following the same procedure for standards and QCs (Scheme S1).

As shown in Table 3, a Pearson coefficient of 0.98 and a mean difference of 5.3% shows a good correlation and accuracy of the SPR assay with respect to HPLC-MS values, as shown also in the histogram in Fig. 5b.

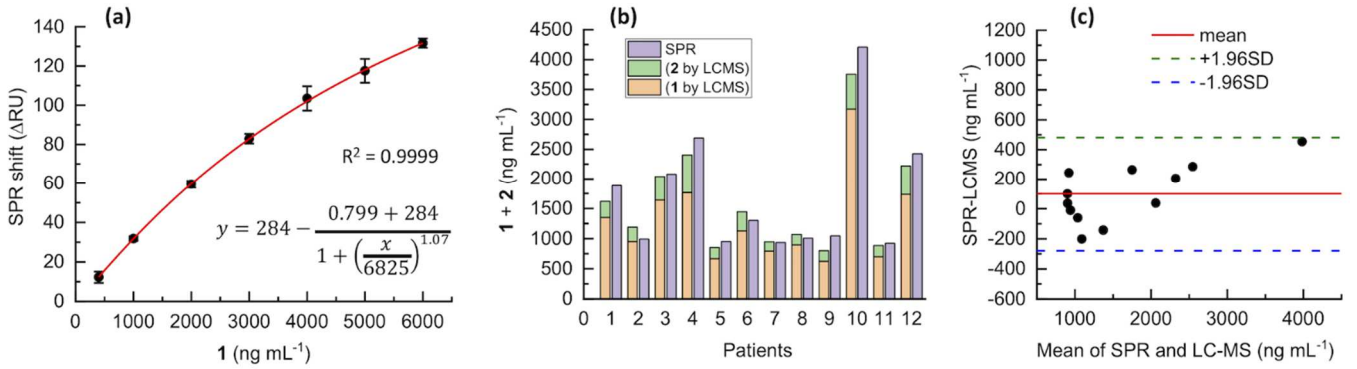

Fig. 5 (a) Calibration curve obtained upon blank subtraction and 4PL regression analysis of three replicates of undiluted plasma sample; (b) histogram showing the comparison of plasma concentration of **1** and **2** detected by SPR and HPLC-MS; (c) Bland-Altman plot showing biases vs HPLC-MS.

Table 3 Summary of comparison data for the SPR assay *vs* HPLC-MS.

patients	HPLC-MS (ng mL^{-1})			SPR (ng mL^{-1})
	1	**2**	total	
1	1354	265	1619	1883
2	950	242	1192	991
3	1643	399	2042	2080
4	1766	638	2404	2689
5	669	184	853	953
6	1130	315	1445	1302
7	792	156	948	937
8	898	171	1069	1008
9	623	177	800	1044
10	3170	586	3756	4210
11	699	188	887	923
12	1736	484	2220	2425
R^2			0.98	
Mean difference			5.3%	

Moreover, although a small sample size was available, an acceptable degree of correlation between the two techniques was obtained by analyzing data with the Bland-Altman plot (Fig. 5c). Considering the preliminary nature of these results, we conclude that a biosensor approach employing aptamers would potentially lead to the development of a reliable analytical tool for TDM of imatinib and, in perspective, of other drugs. This would be beneficial for both the patient outcome and the healthcare system, especially when considering that it would prevent those toxicity events occurring in the case of over dosage, such as thrombocytopenia and hematological Grade 3/4 adverse effects.[14]

Conclusions

In conclusion, we described an SPR investigation employing an aptamer as receptor for the anti-cancer drug imatinib and its main metabolite N-desmethyl imatinib in human plasma. Despite SPR response of small molecules interacting with biomolecular receptors is usually considered challenging due to the low mass change at the sensor surface, we successfully developed a quantitative assay with consistent validation data covering the range of concentrations within the therapeutic window of this drug. The method was then validated and tested on plasma samples with very promising results. A significant outcome of this study is that preparation of clinical samples suitable for the analysis by a biosensing approach required dilution of the samples with aqueous buffers, avoiding the need of organic solvents and denaturing conditions. Furthermore, this work demonstrates that biosensor-based strategies can be implemented to detect and quantify small drug molecules in biological fluids with reliable validation data for clinical analysis, as required by regulatory guidelines. We therefore prospect the possible application of aptamer-based assays to the development of novel analytical tools aimed at monitoring therapeutic drugs in large groups of patients, which are still excluded from TDM practice in clinical oncology.

Conflicts of interest

D. B. is a Co-founder and Director of Aptamer Group and therefore has financial interest in Aptamer Group Ltd.

Acknowledgements

We acknowledge Regione Friuli-Venezia-Giulia trough the POR FESR 2014–2020 (project “Nano Diagnostics and Automated Tools for Oncology”, NADIATools) and the grant AIRC 5X1000 (Rif. 12214) “Application of advanced nanotechnology in the development of innovative cancer diagnostics tools” for financial support.

Notes and references

1 M. Deininger, E. Buchdunger and B. J. Druker, *Blood*, 2005, **105**, 2640–2653.
2 M. D. Moen, K. McKeage, G. L. Plosker and M. A. A. Siddiqui, *Drugs*, 2007, **67**, 299–320.
3 X. Thomas and M. Heiblig, *Expert Opin. Drug Discov.*, 2016, **11**, 1061–1070.
4 T. Kubota, *Int. J. Clin. Oncol.*, 2006, **11**, 184–189.
5 J. F. T. Teng, V. H. Mabasa and M. H. H. Ensom, *Ther. Drug Monit.*, 2012, **34**, 85–97.
6 S. Patel, *Cancer Chemother. Pharmacol.*, 2013, **72**, 277–286.
7 G. D. Demetri, Y. Wang, E. Wehrle, A. Racine, Z. Nikolova, C. D. Blanke, H. Joensuu and M. Von Mehren, *J. Clin. Oncol.*, 2009, **27**, 3141–3147.
8 T. Schindler, W. Bornmann, P. Pellicena, W. T. Miller, B. Clarkson and J. Kuriyan, *Science, 2000, **289**, 1938–1942.*
9 C. Delbaldo, E. Chatelut, M. Re, A. Deroussent, S. Seronie-Vivien, A. Jambu, P. Berthaud, A. Le Cesne, J.-Y. Blay and G. Vassal, *Clin. Cancer Res.*, 2006, **12**, 6073–6078.
10 P. le Coutre, K.-A. Kreuzer, S. Pursche, M. v. Bonin, T. Leopold, G. Baskaynak, B. Dörken, G. Ehninger, O. Ottmann, A. Jenke, M. Bornhäuser and E. Schleyer, *Cancer Chemother. Pharmacol.*, 2004, **53**, 313–323.
11 V. Iacuzzi, B. Posocco, M. Zanchetta, M. Montico, E. Marangon, A. S. Poetto, M. Buzzo, S. Gagno, A. Buonadonna, M. Guardascione, B. Casetta and G. Toffoli, *PLoS One*, 2019, **14**, e0225225.
12 T. Hunter, *J. Clin. Invest.*, 2007, **117**, 2036–2043.
13 P. Herviou, E. Thivat, D. Richard, L. Roche, J. Dohou, M. Pouget, A. Eschalier, X. Durando and N. Authier, *Oncol. Lett.*,

2016, **12**, 1223–1232.

14 R. B. Verheijen, H. Yu, J. H. M. Schellens, J. H. Beijnen, N. Steeghs and A. D. R. Huitema, *Clin. Pharmacol. Ther.*, 2017, **102**, 765–776.

15 N. Guichard, D. Guillarme, P. Bonnabry and S. Fleury-Souverain, *Analyst*, 2017, **142**, 2273–2321.

16 A. Haouala, B. Zanolari, B. Rochat, M. Montemurro, K. Zaman, M. A. Duchosal, H. B. Ris, S. Leyvraz, N. Widmer and L. A. Decosterd, *J. Chromatogr. B Anal. Technol. Biomed. Life Sci.*, 2009, **877**, 1982–1996.

17 N. Widmer, C. Bardin, E. Chatelut, A. Paci, J. Beijnen, D. Levêque, G. Veal and A. Astier, *Eur. J. Cancer*, 2014, **50**, 2020–2036.

18 A. Meneghello, S. Tartaggia, M. D. Alvau, F. Polo and G. Toffoli, *Curr. Med. Chem.*, 2017, **25**, 4354–4377.

19 J. Rodríguez, J. J. Berzas, G. Castañeda and N. Rodríguez, *Talanta*, 2005, **66**, 202–209.

20 J. Rodríguez, G. Castañeda and I. Lizcano, *Electrochim. Acta*, 2018, **269**, 668–675.

21 S. Fornasaro, A. Bonifacio, E. Marangon, M. Buzzo, G. Toffoli, T. Rindzevicius, M. S. Schmidt and V. Sergo, *Anal. Chem.*, 2018, **90**, 12670–12677.

22 Y. Nakano, T. Saita and H. Fujito, *Biol. Pharm. Bull.,* 2013, **36**, 1964–1968.

23 T. Saita, Y. Yamamoto, K. Hosoya, Y. Yamamoto, S. Kimura, Y. Narisawa and M. Shin, *Anal. Chim. Acta*, 2017, **969**, 72–78.

24 A. J. Bonham, K. Hsieh, B. S. Ferguson, A. Vallée-Bélisle, F. Ricci, H. T. Soh and K. W. Plaxco, *J. Am. Chem. Soc.*, 2012, **134**, 3346–3348.

25 A. Vallée-Bélisle, F. Ricci, T. Uzawa, F. Xia and K. W. Plaxco, *J. Am. Chem. Soc.*, 2012, **134**, 15197–15200.

26 A. Porchetta, R. Ippodrino, B. Marini, A. Caruso, F. Caccuri and F. Ricci, *J. Am. Chem. Soc.*, 2018, **140**, 947–953.

27 S. Ranallo, A. Porchetta and F. Ricci, *Anal. Chem.*, 2019, **91**, 44–59.

28 S. Ranallo, M. Rossetti, K. W. Plaxco, A. Vallée-Bélisle and F. Ricci, *Angew. Chemie Int. Ed.*, 2015, **54**, 13214–13218.

29 M. Bhamidipati, H.-Y. Cho, K.-B. Lee and L. Fabris, *Bioconjug. Chem.*, 2018, **29**, 2970–2981.

30 A. Aviñó, A. F. Jorge, C. S. Huertas, T. F. G. G. Cova, A. Pais, L. M. Lechuga, R. Eritja and C. Fabrega, *Biochim. Biophys. Acta - Gen. Subj.*, 2019, **1863**, 1619–1630.

31 N. Fabri-Faja, O. Calvo-Lozano, P. Dey, R. A. Terborg, M.-C. Estevez, A. Belushkin, F. Yesilköy, L. Duempelmann, H. Altug, V. Pruneri and L. M. Lechuga, *Anal. Chim. Acta*, 2019, **1077**, 232–242.

32 M. R. Dunn, R. M. Jimenez and J. C. Chaput, *Nat. Rev. Chem.*, 2017, **1**, 0076.

33 S. Hearty, P. Leonard, H. Ma and R. O'Kennedy, In: Nevoltris D., Chames P. (eds) Antibody Engineering. Methods in Molecular Biology. Humana Press, New York, NY. 2018, **1827**, 421–455. https://doi.org/10.1007/978-1-4939-8648-4_22

34 M. J. Cannon, G. A. Papalia, I. Navratilova, R. J. Fisher, L. R. Roberts, K. M. Worthy, A. G. Stephen, G. R. Marchesini, E. J. Collins, D. Casper, H. Qiu, D. Satpaev, S. F. Liparoto, D. A. Rice, I. I. Gorshkova, R. J. Darling, D. B. Bennett, M. Sekar, E. Hommema, A. M. Liang, E. S. Day, J. Inman, S. M. Karlicek, S. J. Ullrich, D. Hodges, T. Chu, E. Sullivan, J. Simpson, A. Rafique, B. Luginbühl, S. N. Westin, M. Bynum, P. Cachia, Y. J. Li, D. Kao, A. Neurauter, M. Wong, M. Swanson and D. G. Myszka, *Anal. Biochem.*, 2004, **330**, 98–113.

35 A. L. Chang, M. McKeague, J. C. Liang and C. D. Smolke, *Anal. Chem.*, 2014, **86**, 3273–3278.

36 R. Nutiu and Y. Li, *Angew. Chemie Int. Ed.*, 2005, **44**, 1061–1065.

37 R. Stoltenburg, N. Nikolaus and B. Strehlitz, *J. Anal. Methods Chem.*, 2012, 415697, 1–14. https://doi.org/10.1155/2012/415697.

38 E. Barnes, D. Bunka, C. Reinemann, A. Tolley, Patent Application WO2020109791 A1, 2020.

39 Food and Drug Administration, in: Guidance for Industry Bioanalytical Method Validation draft guidance, 2013. http://www.fda.gov/downloads/Drugs/GuidanceComplianceRegulatoryInformation/Guidances/UCM368107.pdf.

40 E. Tenaglia, A. Ferretti, L. A. Decosterd, D. Werner, T. Mercier, N. Widmer, T. Buclin and C. Guiducci, *J. Pharm. Biomed. Anal.*, 2018, **159**, 341–347.

41 B. Peng, P. Lloyd and H. Schran, *Clin. Pharmacokinet.*, 2005, **44**, 879–894.

42 D. H. Josephs, D. S. Fisher, J. Spicer and R. J. Flanagan, *Ther. Drug Monit.*, 2013, **35**, 562–587.

43 B. Peng, M. Hayes, D. Resta, A. Racine-Poon, B. J. Druker, M. Talpaz, C. L. Sawyers, M. Rosamilia, J. Ford, P. Lloyd and R. Capdeville, *J. Clin. Oncol.*, 2004, **22**, 935–942.

44 C. Situ, A. R. G. Wylie, A. Douglas and C. T. Elliott, *Talanta*, 2008, **76**, 832–836.

45 M. Azadeh, B. Gorovits, J. Kamerud, S. MacMannis, A. Safavi, J. Sailstad and P. Sondag, *AAPS J.*, 2018, **20**, 22. https://doi.org/10.1208/s12248-017-0159-4.

46 F. Guilhot, T. P. Hughes, J. Cortes, B. J. Druker, M. Baccarani, I. Gathmann, M. Hayes, C. Granvil and Y. Wang, *Haematologica*, 2012, **97**, 731–738.

